Study of gold nanoparticles and live cells interactions by using planar evanescent wave excitation

Chia-Wei Lee
En-Hong Lin
Ji-Yen Cheng
Academia Sinica
Research Center for Applied Sciences
128, Section 2, Academia Road
Nankang, Taipei 11529
Taiwan

Pei-Kuen Wei
Academia Sinica
Research Center for Applied Sciences
128, Section 2, Academia Road
Nankang, Taipei 11529
Taiwan
and
National Yang Ming University
Institute of Biophotonics Engineering
Taipei, 112
Taiwan

Abstract. We present a planar evanescent wave (PEW) technique combined with phase contrast optical microscopy to study the interactions between cells and gold nanoparticles (AuNPs). The PEW method employs a dual-fiber-line guide to couple light into a thin glass slide. It produces a uniform and long evanescent wave near the glass surface, as verified by the optical near-field measurement. High-contrast AuNP images are obtained by the PEW illumination. At the same time, cells are observed only by using the phase contrast microscopy. The nanoparticles and cell images indicated that unmodified AuNPs had no interactions with cells, possibly due to the negative surface charges on both cells and nanoparticles. The electrostatic concept was further verified by coating AuNPs with positively charged poly (L-lysine). DNA aptamers for surface mucin glycoprotein were coated on AuNPs to demonstrate the application for single nanoparticle tracking.
[DOI: 10.1117/1.3116710]

Keywords: microscopes; scattering; cells; nanoparticles.

Paper 08243SSRR received Jul. 18, 2008; revised manuscript received Feb. 11, 2009; accepted for publication Feb. 11, 2009; published online Apr. 13, 2009.

1 Introduction

Plasmonic metallic nanoparticles, such as gold and silver nanoparticles, are becoming important materials in live cell studies.[1–4] Compared to modern quantum dots, gold nanoparticles (AuNPs) are more biocompatible and less toxic.[5] The surface modification is easy because gold has good affinity to thiol and amine groups. In addition, AuNP has a large absorption in the visible and near-infrared range due to the excitation of localized surface plasmon resonance. When an intense light focuses on the AuNPs, the large optical absorption will increase the temperature of AuNPs. The heating effect of AuNPs can be used for phototherapy.[6] The study of AuNPs and cell interactions requires a real-time and simultaneous observations of nanoparticles and cells. Gold is not fluorescent, but the plasmonic effect causes AuNPs to have a high scattering ability compared to cell organelles. The scattering cross section of a nanoparticle is calculated by[7]

$$C_s(\lambda) = \frac{128\pi}{3\lambda^4} r^6 n^4 \frac{[\varepsilon_r(\lambda) - n^2]^2 + \varepsilon_i^2(\lambda)}{[\varepsilon_r(\lambda) + 2n^2]^2 + \varepsilon_i^2(\lambda)}, \qquad (1)$$

where r is the radius of nanoparticle; λ is the incident wavelength; n is the refractive index of liquid medium; and ε_r and ε_i are the real and imaginary parts of the dielectric constant of the nanoparticle, respectively. When $\varepsilon_r = -2n^2$, the scattering reaches the maximum value. Gold and silver meet this resonant condition in the visible range. They have much higher scattering efficiency compared with other materials, such as aluminum, iron, copper, and titanium oxide. However, silver nanoparticles are highly toxic to cells.[8] Therefore, the scattering of AuNPs is used as a contrast effect for imaging nanoparticles in live cells.

The widely used cell imaging techniques, such as phase contrast (PhC) or differential interference contrast, are operated in the bright-field mode. AuNPs are much smaller than the incident wavelength. It is difficult to see AuNPs by such a transmission setup due to the large background. On the other hand, dark-field techniques such as oblique illumination[9] or confocal optical microscopy[10] have been reported for imaging nanoparticles only. The large difference in the illumination requirements, bright field against dark field, makes simultaneous observations of cells and AuNPs difficult. In this paper, we present a method to overcome the illumination problem by incorporating a planar evanescent wave (PEW) setup into a phase-contrast optical microscope. The PEW is generated on a glass slide. AuNPs near the glass surface scatter the PEW, which yields a very low background nanoparticle image. The proposed PEW setup has several advantages over conventional total internal reflection (TIR) method. It has a uniform distribution of evanescent field. The depth of PEW is much longer and more suitable for observing cells. Most importantly, the PEW setup is easy to incorporate into most optical microscopes. There are two different intensities for the illuminations. Simultaneous cells and AuNP images are obtained by simply adjusting illumination conditions for the bright field and PEW images.

Address all correspondence to: Pei-Kuen Wei, Research Center for Applied Sciences, Academia Sinica, Taipei, 11529, Taiwan. Tel: (886) 2-27898000; Fax: (886) 2-2823-5460; E-mail: pkwei@gate.sinica.edu.tw.

1083-3668/2009/14(2)/021005/6/$25.00 © 2009 SPIE

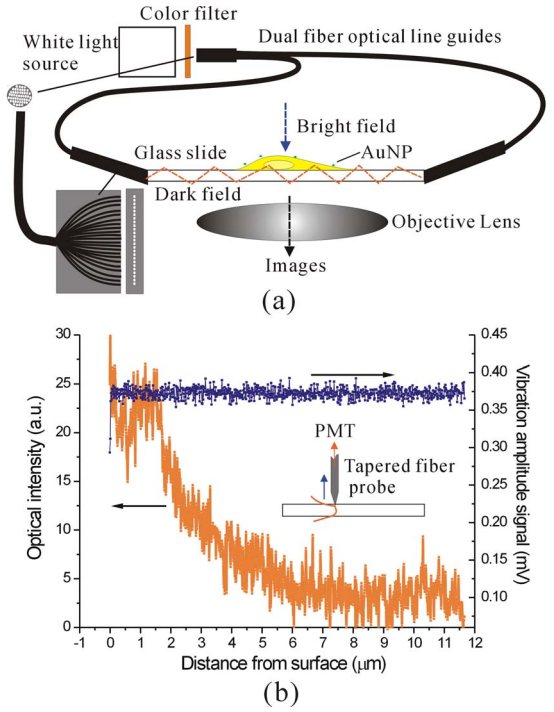

Fig. 1 (a) Schematic of the dual-illumination method. Cell images are taken by the PhC. AuNP images are obtained by scattering the evanescent wave on the glass waveguide. A dual-light line guide coupled light into the glass slide from opposite ends to produce uniform and symmetric evanescent planar wave. (b) PEW intensities and the vibration amplitude signal as a function of distance from the glass surface. The measurements were made using a tapered fiber probe, as shown in the inset. The intensity profile of the PEW shows an exponential decay. The decay length is about 2 μm.

2 Methods

Figure 1(a) illustrates the dual-illumination method for imaging cells and AuNPs. There are two light sources. One is a normally incident light. It interacts with the cells and produces a phase-contrast cell image. The other is a white light, filtered by a color filter to fit the maximum scattering spectrum of AuNPs. The light is coupled to a thin glass slide by using fiber-coupling method. Light propagates along the slide, yielding a uniform distribution of optical field in the glass. From the optical waveguide theory,[11] a uniform evanescent wave exists on the waveguide surface. Such an evanescent wave can not be detected in the far field. But when AuNPs are close to the glass surface, the evanescent wave is scattered to the far field and renders an almost background-free and high-contrast nanoparticle image. In this experimental setup, we used a dual-fiber optical line guide to couple light into opposite ends of the glass slide. The light guide was made from hundreds of optical fibers, which were circularly arranged at the input. At the output, those fibers were rearranged to form two lines. This two-end coupling method makes a symmetric PEW. Note that the line guide had an incident angle of ~20 deg and light from the fibers had a divergent angle of ~30 deg. This results in substantial optical waves propagating near the critical angle (~37.5 deg) of water/glass interface. These critical waves made a long PEW on the glass surface. To verify the depth of the PEW, we used a tapered optical fiber probe to collect intensities at different heights. The fiber probe[12] had a tip smaller than 100 nm. It was vibrated by a small piezoelectric tube. A small tuning-fork was mounted on the probe to measure the vibration amplitude.[13] When the tip touched the glass surface, the tuning-fork sensed a sharp decrease of vibration. It gave a reference for the water/glass interface. The PEW was collected by the fiber probe and sent to a photomultiplier tube (PMT) to measure its optical intensity. Figure 1(b) shows the measured PEW intensities and the vibration amplitude as a function of distance from the glass surface. The intensity profile of the PEW was an exponential decay. The decay length was about 2 μm, which was about one order of magnitude longer than that of conventional TIR method. Note that the "Darklit" system (Micro Video Instruments, Inc.) also couples light from the ends of a glass slide at a zero incident angle. It produces uniform dark illumination for imaging silver grains and immunogold. The proposed setup is aimed for simultaneously observing living cells and AuNps. A PhC setup was combined with the dark-field illumination method. In addition, the PEW excitation has an incident angle close the critical angle of water/glass interface. This results in a longer evanescent tail and is more suitable for imaging micrometer-thick cells.

Figure 2(a) shows the setup of the microscopic system. The light source for the dual-line guide was a 150-W Hg–Xe lamp. An orange color filter was used to match the maximum scattering spectrum of AuNPs. Input of the line guide had a 3 cm diameter, which efficiently coupled the white light source into the fiber bundle. The output was divided into two lines (1×30 mm), which fixed on the opposite ends of the slide. The PEW illumination system was mounted on the stage of an inverted optical microscope (Olympus IX71). When some AuNPs were near the slide surface, the PEW was scattered by the nanoparticles. This scattering effect results in bright diffraction-limit spots.

AuNPs were prepared by reduction of chloroauric acid ($H[AuCl_4]$) solution. Figure 2(b) shows a TEM image for these 13-nm-diam AuNPs. The nanoparticle size is quite uniform. We prepared the AuNP solutions with a concentration of about 5 nM. Cells were the non-small lung cancer cells (CL1-0) and normal lung cells (WI-38). Those cells were cultured on a cleaned glass slide (gold seal) with a thin square glass chamber to hold the medium. The cells were maintained in RPMI (Roswell Park Memorial Hospital) medium (GIBCO) supplemented with 10% FBS (fetal bovine serum) (GIBCO) at 37 °C, 5% CO_2 in a humidified atmosphere. The cells were cultured over 6 h before use to ensure they spread well on the glass slides.

The slides with cells were put on the PEW modified inverted microscope. To maintain the 37 °C environment, we designed a transparent heater by using an indium-tin-oxide (ITO) electrode. The temperature was maintained by controlling the input current into the ITO electrode. Cells were observed by using the phase contrast in the inverted optical microscope. To test the cell viability, we recorded the cell images for 24 h by the microscope. Video 1 shows growth and proliferation of non-small lung cancer cells (CL1-0). These images show cells in the designed chamber have very good viability.

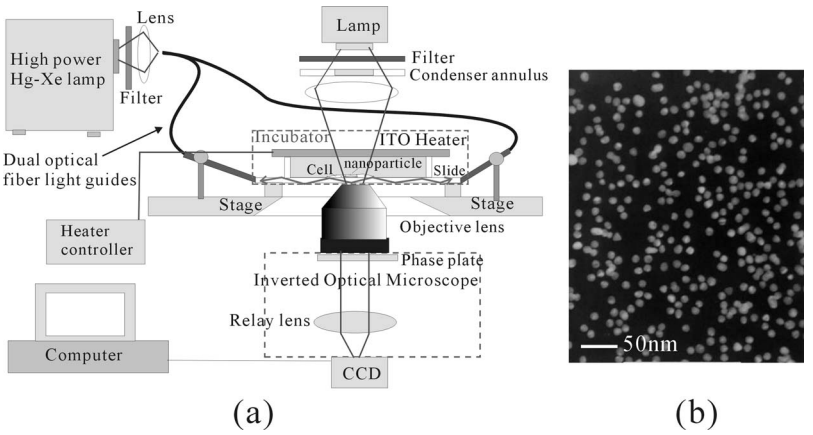

Fig. 2 (a) Optical setup for simultaneous observation of cells and AuNPs. The planar waveguide illumination system was mounted on the stage of an inverted optical microscope. Cells were cultured on the glass slide with a square glass chamber to hold the liquid. The temperature was maintained by controlling the input current into the ITO electrode. (b) The transmission electron microscopy (TEM) image of 13-nm AuNPs.

3 Results and Discussion

Figures 3 show the optical images observed by a 40× objective lens [numerical aperture (NA)=0.6]. Figure 3(a) is the PhC image of lung cancer cells. Clear cell images with mean size about 15 μm were seen. Note that AuNPs were invisible in such bright-field image. Figures 3(b) and 3(c) show the optical images when PEW illumination was turned on. The incubation times for AuNPs in the slide chamber were 20 and 40 min, respectively. Both cells and nanoparticles were seen. It is found that AuNPs without any modification can not attach to the lung cancer cells. Most of the nanoparticles were found on the glass substrate as compared with the cells image. A possible reason for such a nanoparticle distribution is the electrostatic force. In the preparation of AuNPs, the sodium citrate first acts as a reducing agent. Later the negatively charged citrate ions are adsorbed onto the gold nanoparticles, introducing the negative surface charge that repels the nanoparticles and prevents them from aggregating. It is known that the membrane of cancer cells carries negative charges.[14] Therefore, the electroforce expelled most AuNPs from the cells. Most AuNPs were outside the cells. To verify this electrostatic concept, we coated AuNPs with positively charged poly(L-lysine). Amino groups in poly(L-lysine) neutralized negative charges of AuNPs and reduced repulsion with lipo-

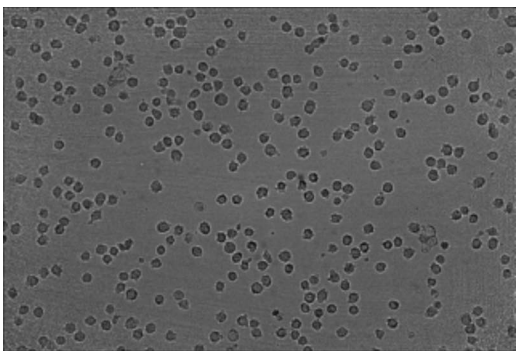

Video 1 Growth and proliferation of non-small lung cancer cells (CL1-0). (Quicktime 1.35 MB).
[URL: http://dx.doi.org/10.1117/1.3116710.1]

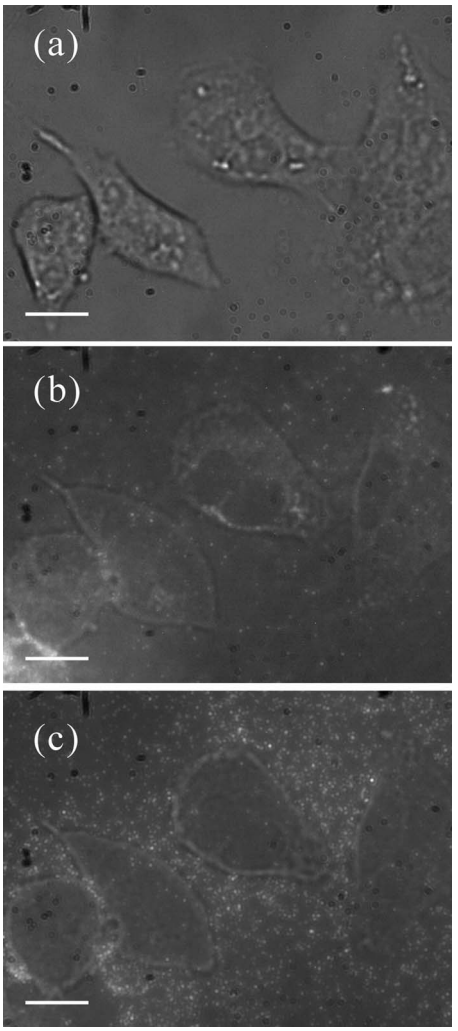

Fig. 3 (a) PhC image of lung cancer cells, AuNPs can not be seen in this bright-field image; (b) 20-min and (c) 40-min interaction times between AuNPs and cells. The optical images were taken by turning on both normal and PEW illuminations. The unmodified AuNPs are outside the cells. The scale bar is 10 μm.

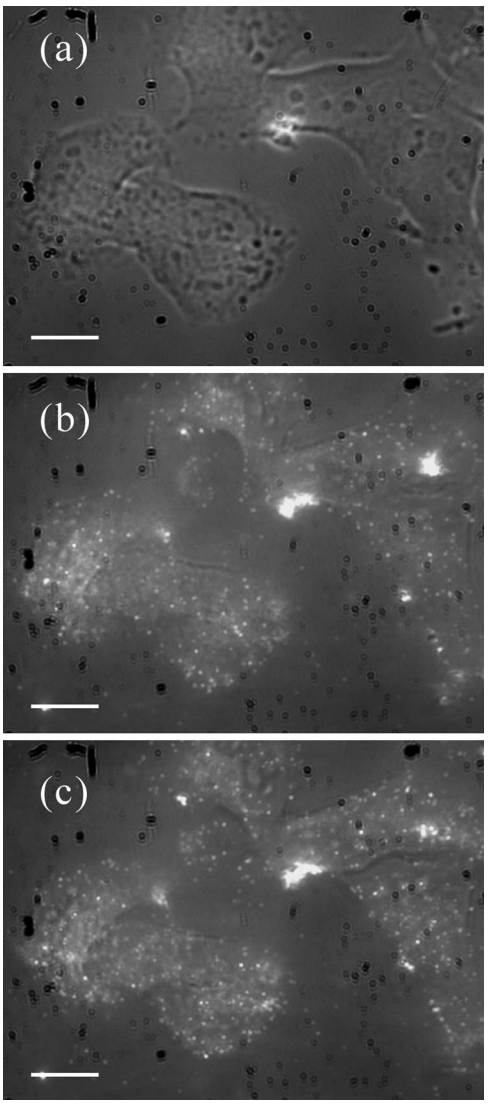

Fig. 4 (a) PhC image of cancer cells and (b) 20 min and (c) 40 min interaction times between AuNPs and cells. The optical images were taken by turning on both normal and PEW illuminations. The AuNPs were coated with poly (L-lysine). Most of the modified AuNPs were found on the cells. The scale bar is 10 μm.

somal membrane. Figure 4(a) is the PhC image of cells. Figures 4(b) and 4(c) are the images when both normal illumination and PEW illumination were turned on. The incubation times for these modified AuNPs in the slide chamber were 20 and 40 min, respectively. Compared with the cells image, most of the poly(L-lysine)-modified AuNPs were attached to the cell membrane.

The cancer cells are easy to culture for their high viability. The system is also useful for normal cells. Figures 5 show the experimental results for normal lung cells (WI-38) observed by a 10× objective lens. Those cells were fibroblasts. They were well attached to the glass surface. Figure 5(a) is the PhC image of a lung normal cell. A clear long cell image was observed. Figure 5(b) shows the image when both normal illumination and PEW illumination were turned on. Compared with the PhC image, many of the AuNPs were attached to the normal cell. The AuNPs were attracted by the normal cell

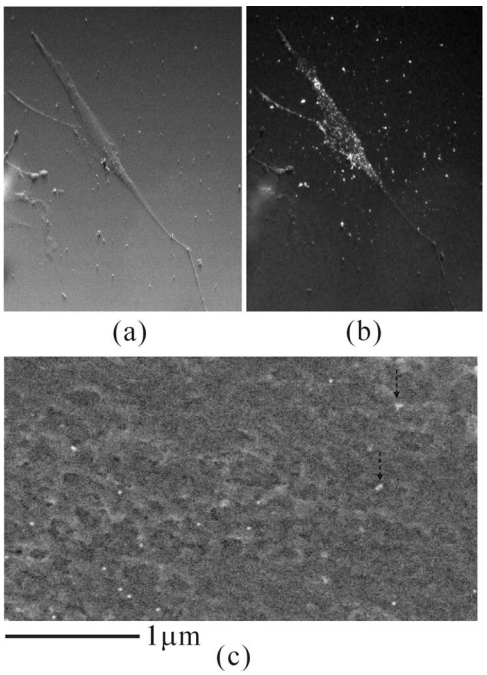

Fig. 5 (a) PhC image of lung normal cells; (b) AuNPs and cell image when both normal illumination and PEW illumination were turned on, compared with the PhC image, many of the poly(L-lysine) modified AuNPs were attached to the normal cell; and (c) the SEM image of AuNPs on the surface of a dried cell. Most particles are single nanoparticles. Few aggregates are indicated by dash arrows.

because of the electrostatic force between poly(L-lysine)-modified AuNPs and cell membrane. It is noticeable that AuNPs are much smaller than the optical resolution. Single nanoparticles and their aggregates can not be verified simply from the particle size. To see the real distribution of nanoparticles, we washed the cell sample with distilled water. AuNPs unbounded from the cell surface were washed away. We then dried the sample in ambient conditions and coated it with a gold thin film (~5 nm) for the observation in a high-resolution scanning-electron microscopy (SEM) image. Figure 5(c) shows the SEM image of AuNPs on the dried cell surface. Most AuNPs are single nanoparticles. Few aggregations were found. Note that AuNPs were clearly found on the membrane surface. If they are internalized by the cell, the nanometer-sized AuNPs should be indistinct due to the coverage of the membrane and other cell organells.

AuNPs attach to the cell membrane when they carry positive charges or are coated with ligands that have strong bioaffinity to membrane receptors. We modified AuNPs with a DNA sequence, 5′-GCAGTTGATCCTTTGGATACCCTGG. This DNA segment is known to be an aptamer[15] for cell surface mucin glycoprotein (MUC1), which is overexpressed in cancerous cells.[16] The designed DNA aptamer has a high bioaffinity to MUC1, therefore the modified AuNPs can attach to the cancer cells through the ligand-receptor interactions. Video 2 shows the interaction between aptamer-modified AuNPs and lung caner cells. In this video, some aptamer-modified AuNPs were captured by the cell. The change of the brightness was due to AuNPs at different heights. There was no quenching in the scattering signal. It is thus feasible to use

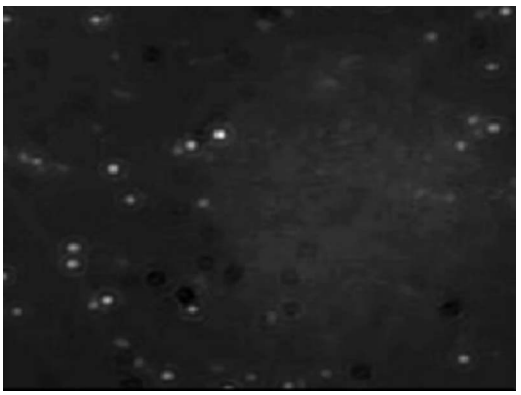

Video 2 Interation between aptamer-modified AuNPs and lung cancer cells. (Quicktime 848.17 KB).
[URL: http://dx.doi.org/10.1117/1.3116710.2]

AuNPs to do the single nanoparticle tracking. Figure 6(a) shows the track of an AuNP that swam around a lung cancer cell and finally immobilized on the cell. For a long interaction time, many AuNPs will be internalized by the cells. Figure 6(b) shows the PhC image of lung cancer cells with aptamer-modified AuNPs. This image was taken by using a 100× oil lens (NA=1.36) after a 2.5-h interaction time. The transmission cell image shows some dark spots that maybe the AuNP aggregates. Figure 6(c) shows the image when both normal illumination and PEW illumination were turned on. Compared with the PhC image, those very bright regions indicated the aggregations of AuNPs. There were some regions with little or no aggregations that can not be seen in the PhC image, but were still clear in the PEW image. Note that the same lung cancer cells were tested with AuNPs without the DNA surface modification. Those unmodified AuNPs have no interactions with cells, as seen in Figs. 3. The uptake of the AuNPs is due to the specific binding between the DNA aptamer and membrane receptors.

The advantage of the PEW method is that it provides a very low background illumination for observing nanoparticles. The conventional dark-field method using oblique illumination has a large scattering background due to the scattering in a large volume of medium. The PEW scatters only objects near the glass surface. Fine structures and nanoparticles near the surface can be clearly seen by this technique. For example, the filopodia of cells adhered very well to the glass substrate. Their image can be enhanced through this PEW illumination, as seen in Fig. 6(c). The filopodia was very small and transparent. It is hardly observed in the conventional bright-field image [see Fig. 6(b)]. Nevertheless, with the PEW method, we can clearly see the distribution of filopodia. Note that this technique can only scatter nanoparticles near the surface. For large cells without good adhesion to the surface, nanoparticles on higher regions of cells can not be detected.

In summary, we presented a method to simultaneously observe cells and AuNPs images. The cell images were taken using a conventional bright-field technique and the nanoparticles were observed by dark-field PEW illumination. We proved that the PEW method generated a long evanescent wave on the glass surface. Symmetrical scattering patterns of

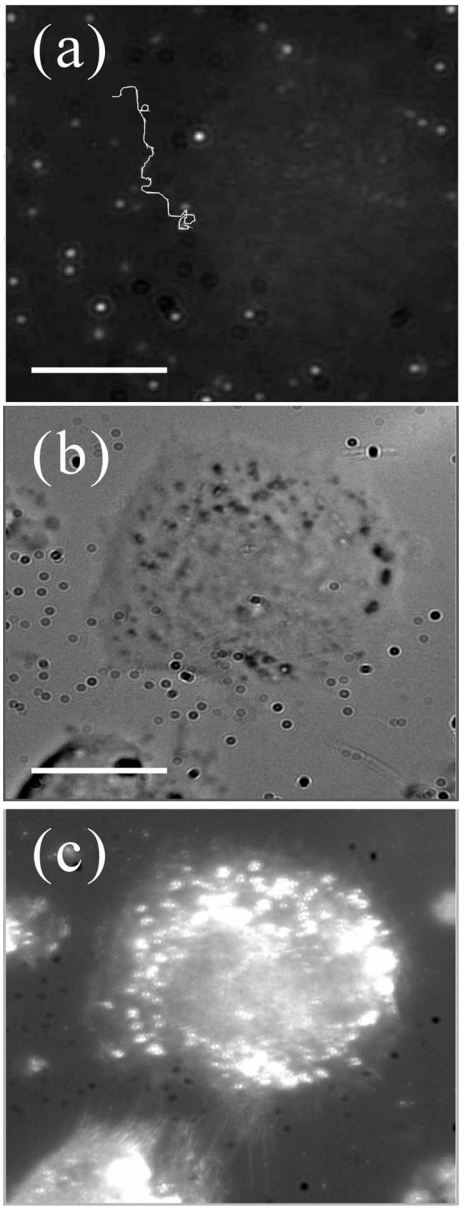

Fig. 6 (a) AuNP image taken by the PEW method only. The bright curve shows the track of an AuNP, which was initially around a cell and finally immobilized. (b) The PhC image of cancer cells with aptamer-modified AuNPs. This image was taken after a 4 h interaction time. (c) The image when both normal illumination and PEW illumination were turned on. Note that the filopodia of the cells were clearly seen in the PEW illumination, but can hardly be observed in the bright-field image. The scale bar is 10 μm.

AuNPs were obtained using a dual-line fiber coupling method. The bare AuNPs were not found on the cancer cells due to the electroexpelling force between the cell membrane and the nanoparticles. With suitable coatings of biomolecules on the AuNP surfaces, the nanoparticles can be immobilized on the cells through the bioaffinity between ligands and membrane receptors. This proposed setup provides a convenient way to observe AuNPs and cells simultaneously. It is very

suitable for single nanoparticle tracking and dynamic studies of nanoparticle-cells interactions.

Acknowledgments

This research is supported by the National Science Council, Taiwan (Grant No. 97-3112-B-001-022) and the Thematic Project of the Academia Sinica, Taiwan.

References

1. A. Wax and K. Sokolov, "Molecular imaging and darkfield microspectroscopy of live cells using gold plasmonic nanoparticles," *Laser Photonics Rev.* **3**, 334–339 (2008).
2. K. S. Lee and M. A. El-Sayed, "Gold and silver nanoparticles in sensing and imaging: sensitivity of plasmon response to size, shape, and metal composition," *J. Phys. Chem. B* **110**, 19220–19225 (2006).
3. I. H. El-Sayed, X. Huang, and M. A. El-Sayed, "Surface plasmon resonance scattering and absorption of anti-EGFR antibody conjugated gold nanoparticles in cancer diagnostics: applications in oral cancer," *Nano Lett.* **5**, 829–384 (2005).
4. L. Cognet, C. Tardin, D. Boyer, D. Choquet, P. Tamarat, and B. Lounis, "Single metallic nanoparticle imaging for protein detection in cells," *Proc. Natl. Acad. Sci.* **100**, 11350–11355 (2003).
5. R. Shukla, V. Bansal, M. Chaudhary, A. Basu, R. R. Bhonde, and M. Sastry, "Biocompatibility of gold nanoparticles and their endocytotic fate inside the cellular compartment: a microscopic overview," *Langmuir* **21**, 10644–10654 (2005).
6. X. Huang, P. K. Jain, I. H. El-Sayed, and M. A. El-Saye, "Plasmonic photothermal therapy (PPTT) using gold nanoparticles," *Lasers Med. Sci.* **23**, 217–228 (2008).
7. M. A. van Dijk, A. L. Tchebotareva, M. Orrit, M. Lippitz, S. Berciaud, D. Lasne, L. Cognet, and B. Lounis, "Absorption and scattering microscopy of single metal nanoparticles," *Phys. Chem. Chem. Phys.* **8**, 3486–3495 (2006).
8. S. M. Hussain, K. L. Hess, J. M. Gearhart, K. T. Geiss, and J. J. Schlager, "In vitro toxicity of nanoparticles in BRL 3A rat liver cells," *Toxicol. In Vitro* **19**, 975–983 (2005).
9. D. A. Schultz, "Plasmon resonant particles for biological detection," *Curr. Opin. Biotechnol.* **14**, 13–22 (2003).
10. K. Lindfors, T. Kalkbrenner, P. Stoller, and V. Sandoghdar, "Detection and spectroscopy of gold nanoparticles using supercontinuum white light confocal microscopy," *Phys. Rev. Lett.* **93**, 037401 (2004).
11. R. G. Hunsperger, *Integrated Optics: Theory and Technology*, 5th ed., Springer, Berlin (2002).
12. P. K. Wei, Y. C. Chen, and H. L. Kuo, "Systematic variation of polymer jacket fibers and the effects on tip etching dynamics," *J. Microsc.* **210**(3), 334–339 (2003).
13. K. Karrai and R. D. Grober, "Piezoelectric tip-sample distance control for near field optical microscopes," *Appl. Phys. Lett.* **66**, 1842–1844 (1995).
14. J. Bauer, *Cell Electrophoresis*, Chap. 14, CRC Press, Boca Raaton, FL (1994).
15. C. S. M. Ferreira, C. S. Matthews, and S. Missailidis, "DNA aptamers that bind to MUC1 tumour marker: design and characterization of MUC1-binding single stranded DNA aptamers," *Tumour Biol.* **27**, 289–301 (2006).
16. J. Taylor-Papadimitriou, J. Burchell, D. W. Miles, and M. Dalziel, "MUC1 and cancer," *Biochim. Biophys. Acta* **1455**, 301–313 (1999).